Acta of Bioengineering and Biomechanics
Vol. 23, No. 2, 2021

Original paper
DOI: 10.37190/ABB-01736-2020-05

Effect of topography parameters on cellular morphology during guided cell migration on a graded micropillar surface

SRIKUMAR KRISHNAMOORTHY[1], HEQI XU[1], ZHENGYI ZHANG[2]*, CHANGXUE XU[1]*

[1] Department of Industrial, Manufacturing, and Systems Engineering, Texas Tech University, Lubbock, Texas, USA.
[2] School of Naval Architecture and Ocean Engineering, Huazhong University of Science and Technology, Wuhan, China.

Purpose: Guided cell migration refers to the engineering of local cell environment to specifically direct cell migration and has important applications such as utilization in cell sorting and wound healing assays. Graded micropillar surfaces have been utilized for achieving guided cell migration. Topographic parameters such as micropillar diameter and spacing gradient may have effects on the morphology of attached cells. It is critical to understand this interaction between the cells and the underlying microscale structures. *Methods:* In this study, a graded micropillar substrate has been fabricated to investigate the effects of the microtopography on the cell morphology in terms of the cell aspect ratio and cell circularity. *Results:* It is found that 1) with the increase of the micropillar diameter, the cell aspect ratio has no significance change. At the small spacing gradients, the aspect ratio is smaller than that at the large spacing gradients; 2) statistical analysis shows both the micropillar diameter and spacing gradient have no significant effect on the cell aspect ratio compared to the flat surface; 3) the cell circularity at the small micropillar diameters is higher than that at the large micropillar diameters. The cell circularity at the micropillar gradient of 0.1 μm is higher than those at the other micropillar gradients; 4) three microtopographic conditions are considered to have statistically significant effect on the cell circularity compared to the flat surface, including the micropillar diameters of 5 μm and 10 μm and the spacing gradient of 0.1 μm.

Key words: c*ell morphology, guided cell interaction, microtopography, graded micropillar*

1. Introduction

The utilization of the local environment to control cell behaviors is a phenomenon with various potential applications. For instance, cell guidance, which refers to the tuning of local cell environment to specifically direct cells, has been used in applications such as the soring of cells [16], wound healing [14], and the diagnosis and treatment of specific infections and injuries [6]. The reconstruction of entire tissues such as corneal substitutes and vascular grafts has been performed *in vitro* by the utilization of topographical substrates to enable cell guidance. Similarly, the modification of the local environment has also been utilized to enable the self-assembly of cells by controlling their adhesion and differentiation [19].

The interaction between cells and the local environment mainly occurs via biological features of the cells, the filopodia and lamellopodia, which are protrusions on the plasma membrane incorporating a large amount of actin [10]. These filopodia are localized at the leading cell edge and use the mechanism of contact angle sensing to probe the microenvironment. Different sizes of topographical features have been reported to have different effects on cell behaviors. For instance, at that nanoscopic scale, the subcellular mechanisms (e.g., neurite sensing and filopodial orientation) are primarily affected [4], and at the microscopic scale, the local topography has effects on the whole cell behav-

Corresponding authors: Zhengyi Zhang, School of Naval Architecture and Ocean Engineering, Huazhong University of Science and Technology, Wuhan 430074, China. Phone: +86 (027) 87543158, e-mail: zhengyizhang@hust.edu.cn; Changxue Xu, Department of Industrial, Manufacturing, and Systems Engineering, Texas Tech University, Lubbock, Texas, 79409, USA. Phone: 806-834-6014, e-mail: changxue.xu@ttu.edu

Received: October 16th, 2020
Accepted for publication: April 16th, 2021

iors, such as cell morphology [15]. The extracellular matrix (ECM) is a complex meshwork that is present within all biological structures, such as organs and tissues, which functions as a framework to connect cells together. The ECM has been observed to be critical for the regulation of cell behaviors such as morphogenesis, differentiation, and homeostasis in organisms [7]. The ECM is mainly comprised of collagen fibers with a range of diameters from 1–25 μm [5]. Thus, it is important to understand the effects of microscale ECM geometries on the cell behaviors.

Recent studies have established a specific mechanism of cell interaction with topographic features for guided cell migration, termed topotaxis [18]. Primarily, the filopodia of cells tend to sense the cell contact area, and orient and direct the cells towards an optimal zone where the cells can possess a greater cell contact area. Typically, cells tend to migrate towards the sparse fiber zone from the dense fiber zone in order to maximize the cellular contact area with the ECM [18]. Multiple studies have reported the cell behaviors due to topography sensing, with an emphasis on the migration properties. For example, anisotropic nanotopographic surface gradients were shown to influence the cell shape and migration of 3T3 fibroblasts [11]. Specifically, it was observed that along sparse gradients of a graded nanogroove surface, cells tended to orient themselves randomly similarly to cells adhered on flat non-graded surfaces, while on dense gradients, cells were shown to elongate longer along the direction of the grooves. Park et al. [17] reported that invasive and non-invasive melanoma cancer cells tended to exhibit the migration in opposite directions, due to differences in their relative stiffness. The interaction of MC3T3-E1 osteoblast cells with response to micropillars was investigated by Hui et al. [9], and they noted an increase in migration speed of cells when the spacing between micropillars was increased. The effect of anisotropically stiff micropillars on cell morphology and elongation was demonstrated by Alapan et al. [1], and the preferential elongation of cells along the stiffer areas was reported.

The interaction between cells and the ECM is critical for understanding tissue development and regeneration. Prior studies have focused mainly on effect of topography on cell migration properties such as migration speed. However, at the microscopic scale, effect of the local topography on the cell morphology is still missing. Thus, it is very important to understand the interaction between the cells and the microscale structures in terms of cell morphology. In this study, a graded micropillar substrate has been fabricated to mimic the fiber of ECM. The objective of this paper is to study the effect of graded microscale structures on cell morphological features. This paper is organized in the following manner. First, the experimental materials and methods are introduced in detail. Second, the effects of micropillar diameter and micropillar gradient on cell aspect ratio and circularity are studied. Finally, the major conclusions from the study are listed.

2. Materials and methods

2.1. Micropillar substrate fabrication

The natural ECM is typically represented by three types of topographic features, including posts, pits, and grooves. Micropost arrays possess high sensitivity to the contractility of cells, and the tuning of geometric parameters, such as the diameter and the post-spacing gradient, can result in the tailoring of substrate stiffness [2]. The fabrication of microtopographic surface is a combination of a maskless lithography technique and capillary molding method. The lithography technique is utilized to make the silicon master mold. The materials used are a negative photoresist (SQ-10, KemLab, Woburn, MA), a silicon wafer (University-Wafer, Inc., Boston, MA), and a chemical developer (HARE SQ Developer, KemLab, Woburn, MA). In the capillary molding, the materials used are polydimethylsiloxane elastomer (PDMS, Sylgard 184, Dow Corning, Midland. MI), and gelatin (Gelatin Type A, MP Biomedicals, LLC, Solon, OH).

The micropillar substrate was fabricated using the following highlighted in Fig. 1. The silicon wafer with a diameter of 4 inches was coated with a 30-μm layer of the photoresist using a spin coater. The coated silicon wafer was exposed to a UV source with a wavelength of 385 nm and an intensity of 500 mW/cm^2 in the maskless lithography machine (Durham Magneto Optics ML3, Durham, UK). Then, the silicon wafer was subjected to a post-exposure baking and development process using the chemical developer for 2.5 minutes, which resulted in the silicon master mold. The PDMS was coated on the silicon master mold to make the PDMS patterns using the capillary molding at 65 °C for 4 hours. Finally, two-step surface treatment was utilized on the PDMS micropatterns in order to facilitate the proper attachment of cells. The surface treatment process includes corona arc discharge and coating of a gelatin layer using the 0.1% (w/v) gelatin solution.

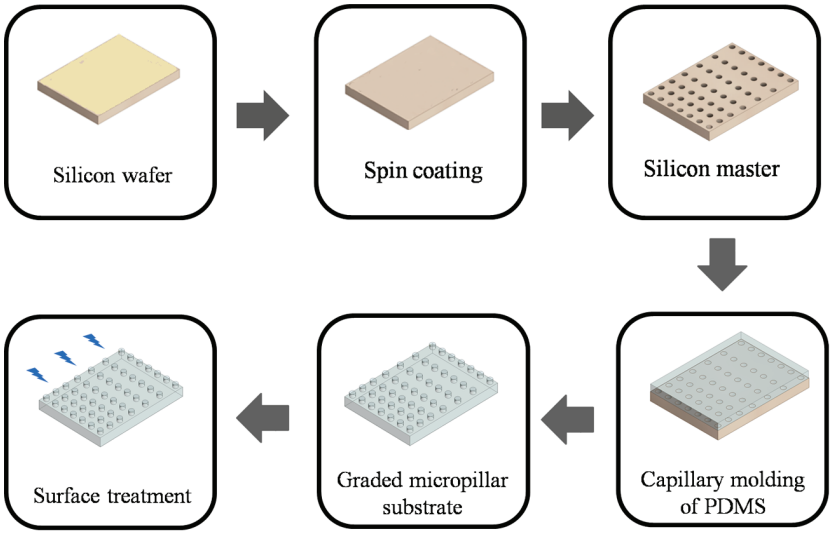

Fig. 1. Fabrication of graded micropillar substrate

2.2. Cell culture and seeding

In this study, fibroblasts were used as the model cells, due to their wide utilization in a variety of applications in 3D bioprinting [12], tissue engineering and regeneration [22], and cell migration studies [21]. NIH 3T3 mouse fibroblasts (ATCC, Rockville, MD) were cultured inside a humidified 5% CO_2 incubator at 37 °C in Dulbecco's Modified Eagles Medium (DMEM; Sigma-Aldrich, St. Louis, MO) supplemented with 1% antibiotic/antimycotic solution (Corning, Manassas, VA) and 10% fetal bovine serum (FBS; HyClone, Logan, UT). Prior to usage in the study, the detachment of cells was performed by the addition of 0.25% Trypsin/EDTA (Sigma-Aldrich, St. Louis, MO) at 37 °C for 3 minutes. The cell suspension was centrifuged at 1000 rpm for 5 minutes. The resultant cell pellet was resuspended in the cell culture medium at a cell concentration of 1×10^5 cells/cm^3. Cell seeding on the micropatterns was performed by adding 0.1 cm^3 of the bioink on the fabricated micropillar substrate followed by incubation for twelve hours at 37 °C to facilitate cell attachment. Further details regarding cell culture procedures can be obtained from our earlier paper [23].

2.3. Morphology characterization

The cells were fixed and permealized using 4% formaldehyde (Santa Cruz Biotechnology Inc., Dallas, TX), which was followed by the staining of the membrane with phalloidin (Santa Cruz Biotechnology Inc., Dallas, TX) and the staining of the nucleus with 4′-6-diamidino-2-phenylindole (DAPI) (Santa Cruz Biotechnology Inc., Dallas, TX). Imaging was then performed using a fluorescence microscope (EVOS FL, Thermo Fisher Scientific, Waltham, MA). The cell images were viewed and assessed using the software ImageJ developed by the National Institutes of Health. Specifically, the cell aspect ratio and circularity were measured and compared on the sparse side and the dense side. The aspect ratio is defined as the ratio of the major axis to the minor axis of the cells. The cell circularity is the ratio of the area of the cells and the area of a circle that has the same perimeter of the cells. Mathematically, the cell aspect ratio is calculated using the following equation [15]:

$$AR = \frac{y}{x},$$

where AR is the cell aspect ratio, y is the length of the cell major axis or the longest length of the cell, and x is the length of the cell minor axis or the length of the cells in the perpendicular direction to the cell major axis. The cell circularity is calculated using the following equation [15]:

$$C = \frac{4 \cdot \pi \cdot A}{p^2},$$

where C is the cell circularity, A is the area of the cell, and p is the cell perimeter. Cell circularity reflecting the shape of the cells is influenced by the cytoskeleton of cells which reorganizes based on the microenvironment (in this case, topography of substrates). A circularity of 1 implies that the cells have not attached, and there is no cytoskeletal reorganization. Lower cell circularities imply that there has been

some cytoskeletal reorganization of cells resulting in less circular shapes.

The geometric parameters influencing the cell morphology on the graded micropillar substrate are the diameter of the micropillars and the micropillar spacing gradient. This study focused on the effects of the micropillar diameter and spacing gradient on the cell aspect ratio and circularity. The micropillar diameter ranged from 5 to 20 μm with an interval of 5 μm, and the micropillar spacing gradient ranged from 0.1 to 0.4 μm with an interval of 0.1 μm. In the vertical direction, the space between the adjacent micropillars was constant at 2 μm. In the horizontal direction, the space between the adjacent micropillars was changing with a spacing gradient of 0.1–0.4 μm. The minimum starting space was 2 μm, and it increased by 0.1–0.4 μm for each row of the rest from the left to the right. The cell aspect ratio and circularity on the graded micropillar substrate were compared with those on the flat surface. One-way ANOVA was used to characterize the significance, and 40 data points were used in each case.

3. Results

In Figure 2a, the fabricated graded micropillar substrate as well as the zoom-in view of individual micropillars are shown. The micropillar diameter is 10 μm, and the micropillar spacing gradient is 0.1 μm. The left side is the dense zone where the micropillars are closer with each other. The right side is the sparse zone where the micropillars are further away from each other. It can also be seen in Fig. 2b that the cells are successfully seeded on the graded micropillar surface. The preliminary results presented in Fig. 3 have demonstrated that the cells can sense the topographic gradient and migrate from the sparse zone to the dense zone. At 0 hours, 52% of cells were in the sparse zone, and 48% of cells were in the dense zone. The cells were randomly seeded on the graded micropillar substrate. However, at 12 hours, only 21% of cells were in the sparse zone, while 79% of cells were in the dense zone.

This paper focuses on cell morphology on the graded micropillar substrate in terms of the cell aspect ratio and circularity. Specifically, Section 3.1 investigates the effects of the micropillar diameter and spacing gradient on the cell aspect ratio. Section 3.2 investigates the effects of the micropillar diameter and spacing gradient on the cell circularity. The cell aspect ratio and circularity on the graded micro-

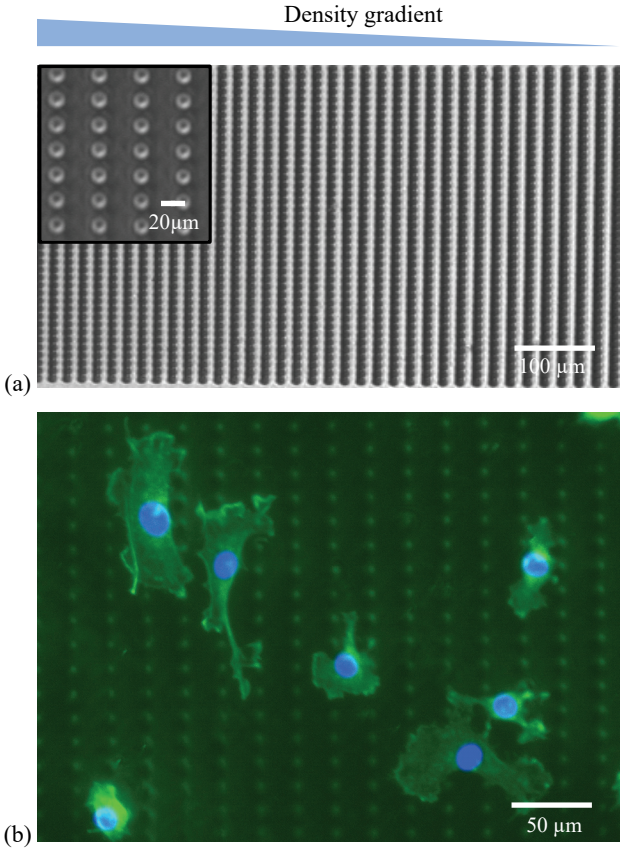

Fig. 2. (a) Fabricated graded micropillar substrate and (b) representative cells attached on the substrate

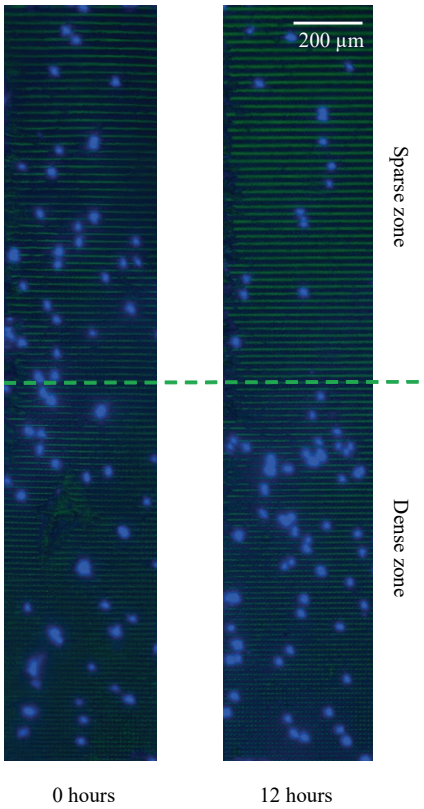

Fig. 3. Demonstration of cell migration from the sparse zone to the dense zone on the graded micropillar substrate

pillar substrate were compared with those on the flat surface to evaluate the cell attachment. The micropillar diameter ranged from 5 to 20 μm with an interval of 5 μm, and the micropillar spacing gradient ranged from 0.1 to 0.4 μm with an interval of 0.1 μm. The micropillar height was fixed as 30 μm. The minimum micropillar spacing was 2 μm, and the maximum micropillar spacing was 12 μm. The average contact areas for individual pillars with different pillars were 78.5 μm^2 for 5 μm, 314.2 μm^2 for 10 μm, 706.7 μm^2 for 15 μm, and 1256.6 μm^2 for 20 μm. Each cell is an individual single cell without contact with other cells.

3.1. Cell aspect ratio

The cell aspect ratio is defined as the ratio of the longest length of the cell and the length of the cell in the perpendicular direction to the major axis. Typically, a higher aspect ratio indicates a greater elongation in the cell morphology [15]. For the fibroblasts, the aspect ratio has been utilized to evaluate the attachment of the cells to the substrate. The higher aspect ratio of the cells indicates a greater level of adhesion to the substrate. This is due to cellular elongation being preceded by the alignment of focal adhesions to the substrate with a greater number of adhesion sites along a particular direction resulting in the greater polarization and elongation of cells [20].

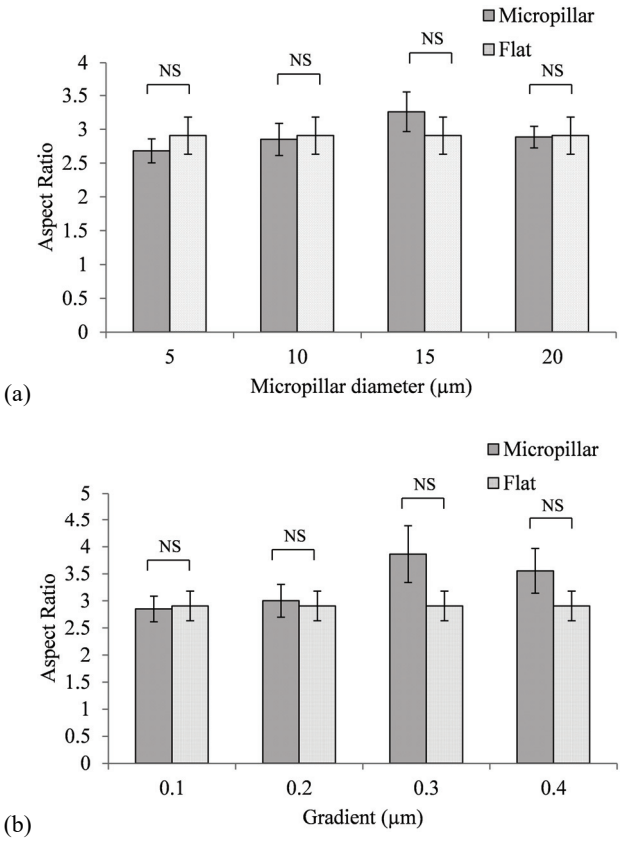

Fig. 4. Effects of (a) micropillar diameter and (b) micropillar spacing gradient on aspect ratio

In Figure 4, the comparison of the cell aspect ratio between the graded micropillar substrate and flat surface is shown. In Figure 4a, the effect of the micropillar diameter on the cell aspect ratio is shown. It can be seen that the cell aspect ratios are 2.7 for the micropillar diameter of 5 μm, 2.8 for the micropillar diameter of 10 μm, 3.3 for the micropillar diameter of 15 μm, and 2.8 for the micropillar diameter of 20 μm, respectively. With the increase of the micropillar diameter, the cell aspect ratio is in the range of 2.7–3.3. The cell aspect ratio on the flat surface is also measured to be of 2.9, which is similar to reported aspect ratio values for 3T3 fibroblasts [3].

It can be seen from Fig. 4a that the cell aspect ratio on the graded micropillar surface is similar to that on the flat surface. One-way ANOVA was used to compare the average aspect ratios on the micropatterned surface and on the flat surfaces. For an assumed alpha level of 0.05, there was no significant difference observed between the average aspect ratios on the patterned surfaces and the flat surfaces. This indicates a consistent level of attachment on the graded micropillar substrate. In addition, in Fig. 5, the frequency distribution of the aspect ratio of cells on various micropillar diameters is listed. It can be seen that in all cases, the majority of cells have aspect ratios in the range of 1–4.

In Figure 4b, the effect of the micropillar gradient on the cell aspect ratio is shown. It can be seen that the aspect ratio at the small spacing gradients is smaller than that at the large spacing gradients. For instance, the cell aspect ratios at the micropillar spacing gradients of 0.1 μm and 0.2 μm are 2.8 and 3.0, while at the micropillar spacing gradient of 0.3 μm and 0.4 μm they are 3.8 and 3.6. The top of the micropillars is the potential focal adhesion point for cells. When the micropillar spacing gradient is smaller, the number of micropillars per unit area is larger, which provides more adhesion points for the cells to attach well. However, when the spacing gradient is larger, the number of micropillars per unit area is smaller, which may require the cells to elongate more, in order to properly attach to an adhesion point. Thus, there is a larger aspect ratio for the larger micropillar spacing gradients. It can be seen from Fig. 4b that the cell aspect ratio at various micropillar spacing gradients is similar to that on the flat surface.

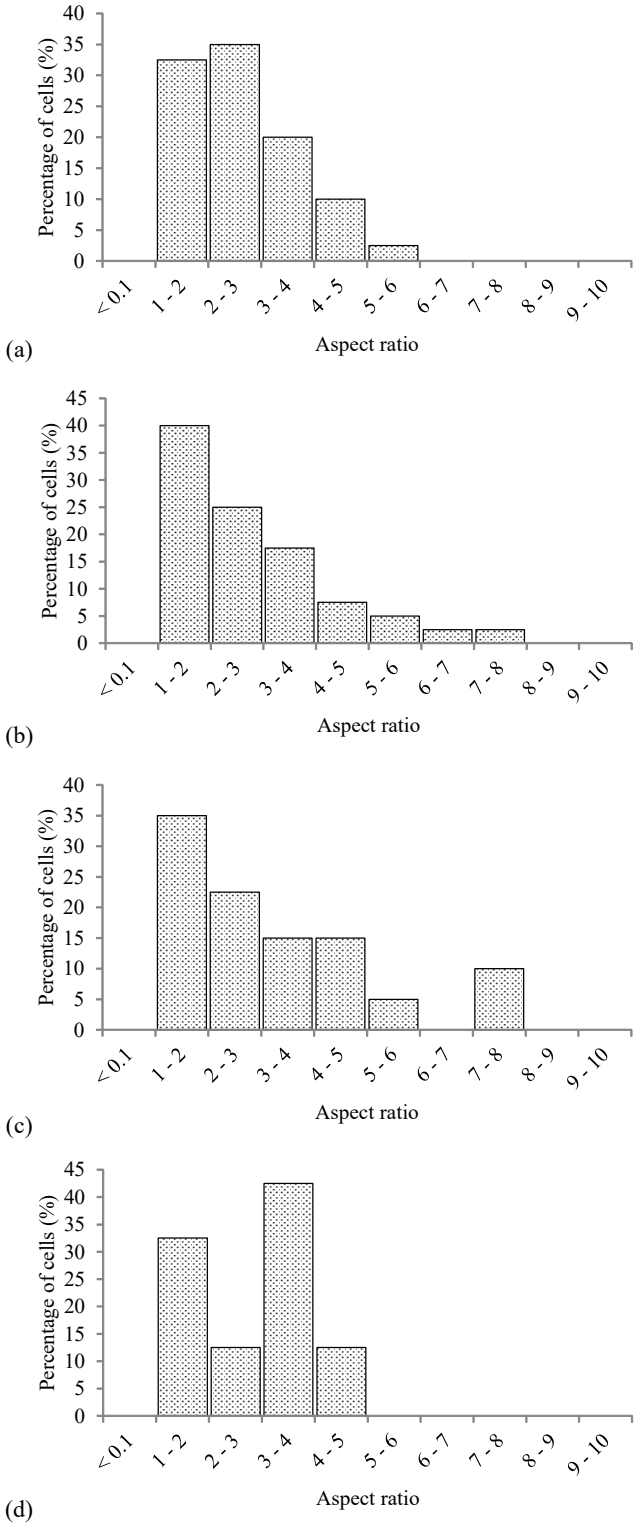

Fig. 5. Frequency distribution of aspect ratios for: (a) 5 µm (SD: 1.13), (b) 10 µm (SD: 1.5), (c) 15 µm (SD: 1.9) and (d) 20 µm micropillar diameters (SD: 1.02)

In Figure 6, the representative cells on these two zones are shown. On the sparse zone, the cell polarization angle is 26°, while on the dense zone the cell polarization angle is 60°. However, the illustrated cells have similar aspect ratios of 2.9 in the dense zone and 3.3 on the sparse zone, in spite of vastly different cell orientations.

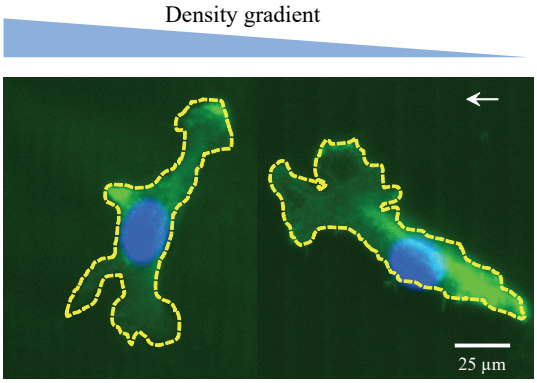

Fig. 6. Cell from the dense zone and sparse zone from a graded micropillar substrate with aspect ratios of 2.9 and 3.3, respectively

3.2. Cell circularity

The cell circularity is defined as the ratio of the area of the cells and the area of a circle that has the same perimeter of the cells. This section focuses on the effects of the micropillar diameter and spacing gradient on the cell circularity on the graded micropillar substrate. The micropillar diameter ranges from 5 to 20 µm with an interval of 5 µm, and the micropillar spacing gradient ranges from 0.1 to 0.4 µm with an interval of 0.1 µm. In Figure 7, the representative cell morphologies at different micropillar diameters of 5–20 µm are shown. The outline of the cells is marked.

In Figure 8, the effect of the microtopography on the cell circularity on the graded micropillar substrate and the flat surface is shown. In Figure 8a, the effect of the micropillar diameter on the cell circularity is shown. It can be seen that the cell circularity at the small micropillar diameters is higher than that at the large micropillar diameters. At the micropillar diameters of 5 µm and 10 µm the cell circularities are 0.45, while they are 0.34 and 0.29 at the micropillar diameters of 15 µm and 20 µm. The cells at the small micropillar diameters are more rounded, while they are more elongated at the large micropillar diameters. This is due to a less available attachment area on the top of the small micropillars. The larger micropillars thus offer a greater focal adhesion area, which may result in better attachment and reduced circularity. The average contact area of individual micropillars increases significantly from 78.5 µm^2 for 5 µm micropillars to 1256.6 µm^2 for 20 µm micropillars.

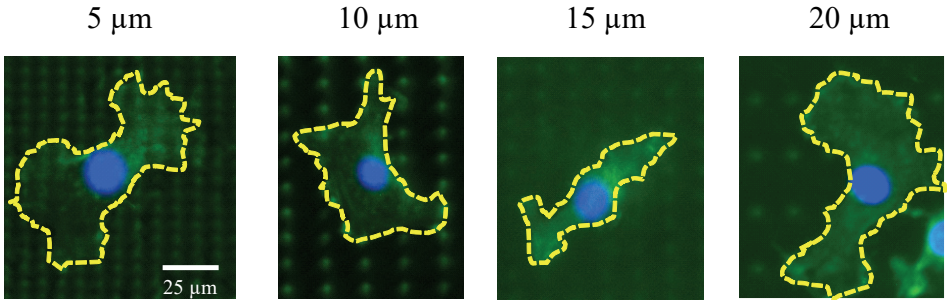

Fig. 7. Representative cell morphologies on the grade micropillar substrates with different micropillar diameters. The circularity values are 0.45, 0.48 0.38, and 0.37 for the micropillar diameters of 5, 10, 15, and 20 µm, respectively

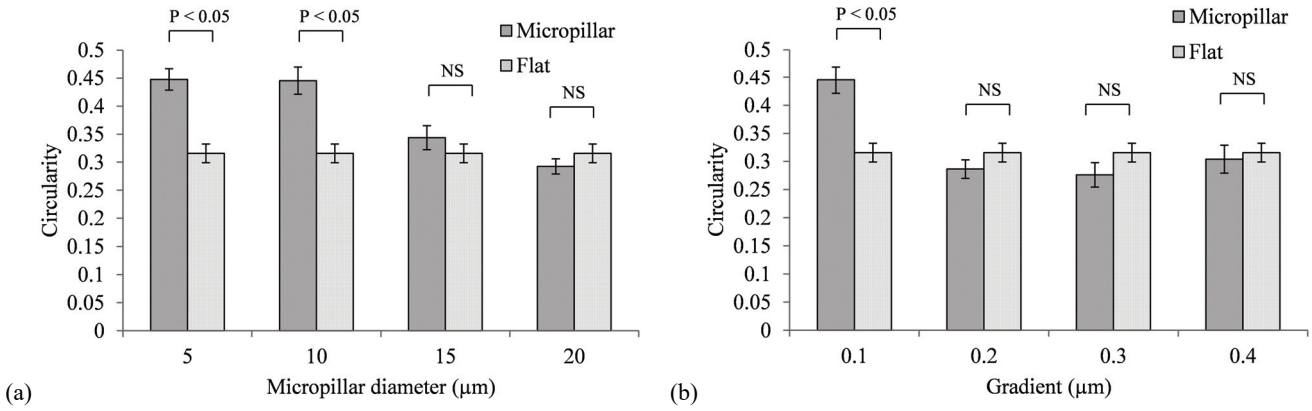

Fig. 8. Effects of (a) micropillar diameter and (b) micropillar spacing gradient on cell circularity

In Figure 8b, the effect of the micropillar spacing gradient on the cell circularity is shown. It can be seen that the cell circularity at the micropillar gradient of 0.1 µm is higher than those at the other micropillar gradients. At the micropillar spacing gradient of 0.1 µm, the cell circularity is 45%. However, the cell circularity at the micropillar spacing gradients of 0.2–0.4 µm is only 28–30%. Moreover, one-way ANOVA was used to compare the cell circularities on the graded micropillar surface and the flat surface. It is found that the micropillar spacing gradient of 0.1 µm causes a statistically significant increase in the circularity compared to the flat surface, while the micropillar substrates with other spacing gradients of 0.2–0.4 µm are statistically identical to the flat substrate. It is probably because of physiological sensing limit of the cells to the underlying topographic gradient. For instance, some earlier studies have indicated the limits of gradients that cells can sense and react appropriately, such as for cell migration [8]. Different cell types have demonstrated to react to different gradients, indicating a fundamental biological difference in sensitivity between various cell types [17]. In this study, the 3T3 fibroblasts seem to be very sensitive to a spacing gradient of 0.1–0.2 µm, above which there is minimal effect on cell attachment.

In Figure 9, a frequency distribution of the cell circularities at different micropillar diameters is shown. It can be seen that for the smaller micropillar diameters of 5 µm and 10 µm, the most frequency of the cell circularities is in the range of 0.4–0.5, while for the larger micropillar diameters of 15 µm and 20 µm, the most frequency of the cell circularities occurs between 0.2–0.3. Moreover, the distribution of the cell circularities is preferentially to the smaller levels with the increasing diameter, indicating that increasing the diameters may induce larger elongation in the attached cells. For example, at the micropillar diameter of 5 µm, around 45% of the cells have circularities of 0.4–0.5. At the micropillar diameter of 10 µm, this decreases to around 30%. At the micropillar diameter of 15 µm, over 35% of the cells have circularities of 0.2–0.3, which increases to 70% for the micropillar diameter of 20 µm. At the spacing gradient of 0.1 µm, the cell circularity is considered as significantly different from that on the flat surface. The graded micropillar substrate has two zones: sparse zone and dense zone. Typically, the cells migrate from the sparse zone to the dense zone. The cell circularities in the sparse and dense zones are compared and are very close. The average cell circularities are 0.46 in the sparse zone and 0.44 in the dense zone. Hence, the spacing dis-

tance between the adjacent micropillars has a negligible effect on the cell circularity. In Figure 10, the frequency distribution of the cell circularity at different spacing gradients is shown. It can be seen that for all the spacing gradients, the distribution in circularities is similar, with the most frequency of cell circularity in 0.2–0.3. In Figure 11, the frequency distribution of the cell circularities on both zones is presented. It can be seen that both distributions are similar, and the most frequency of the cell circularities is 0.2–0.3.

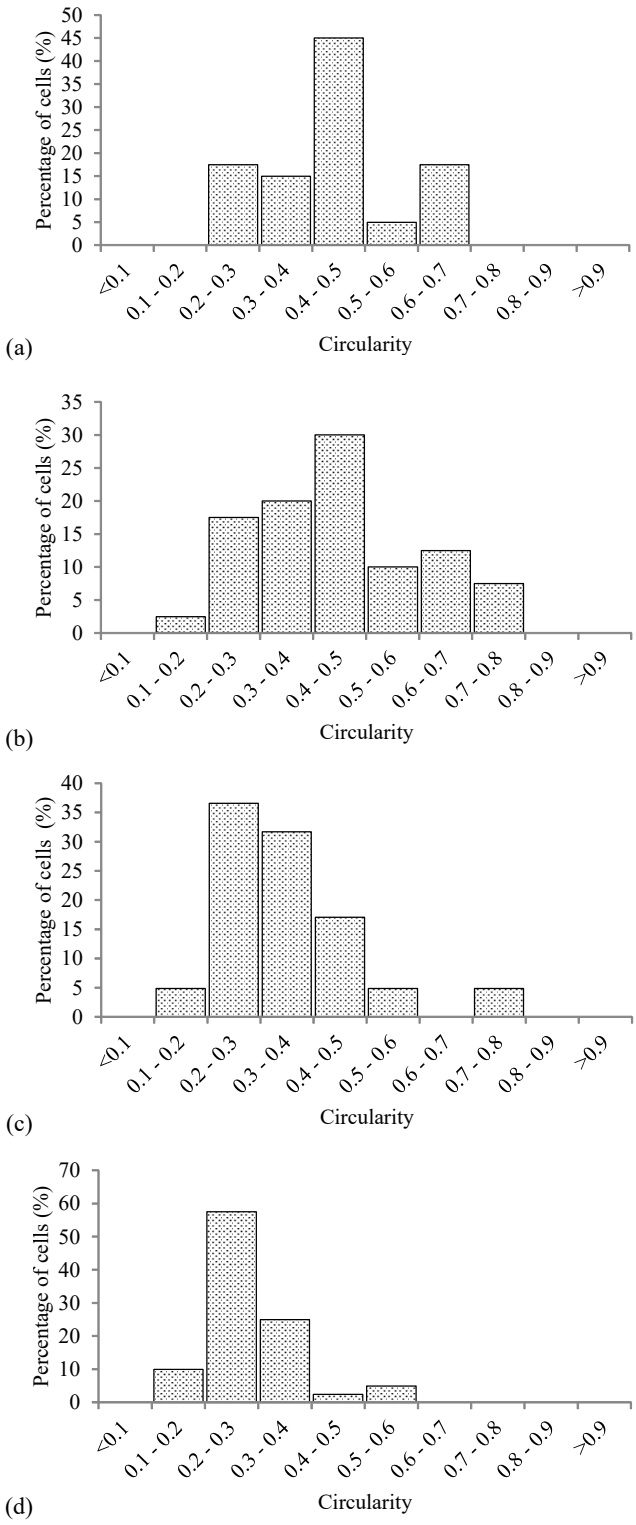

Fig. 9. Frequency distribution of cell circularities for (a) 5 μm (SD: 0.12), (b) 10 μm (SD: 0.12), (c) 15 μm (SD: 0.14), and (d) 20 μm micropillar diameters (SD: 0.08)

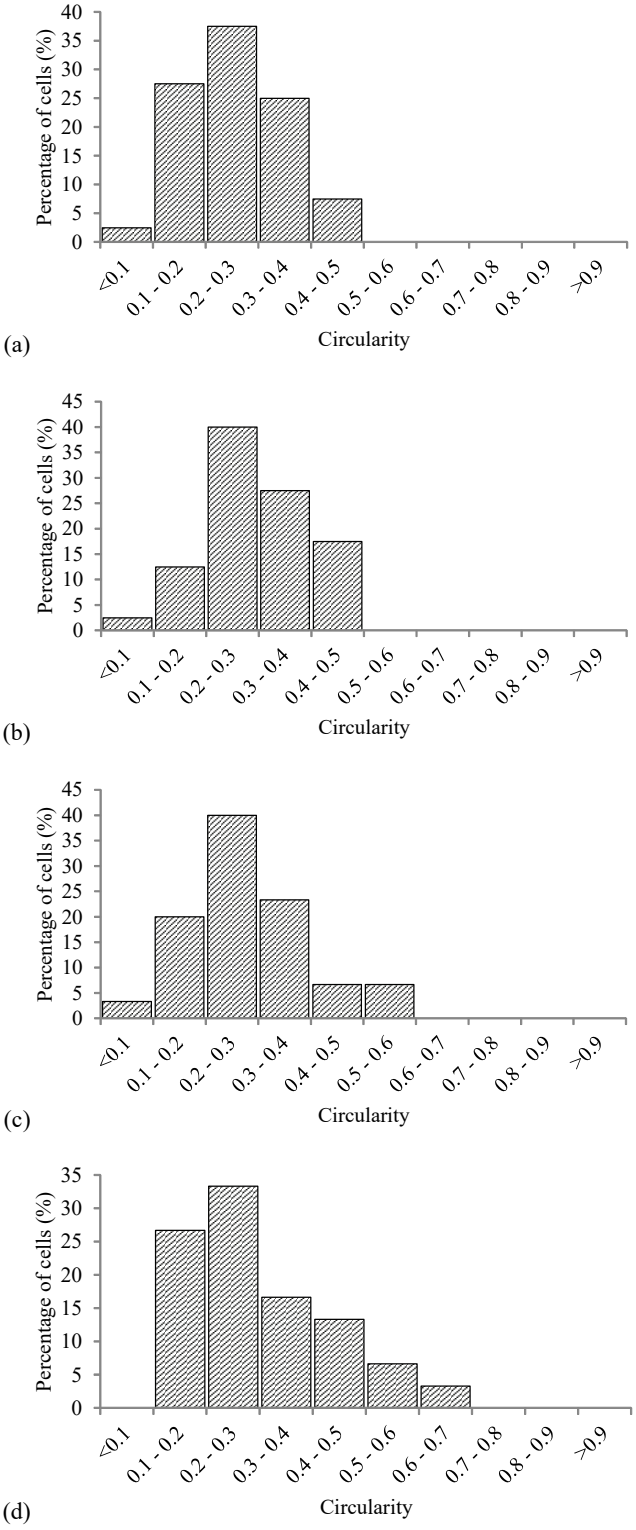

Fig. 10. Frequency distribution of cell circularities for (a) 0.1 μm (SD: 0.09), (b) 0.2 μm (SD: 0.1), (c) 0.3 μm (SD: 0.12), and (d) 0.4 μm spacing gradients (SD: 0.14)

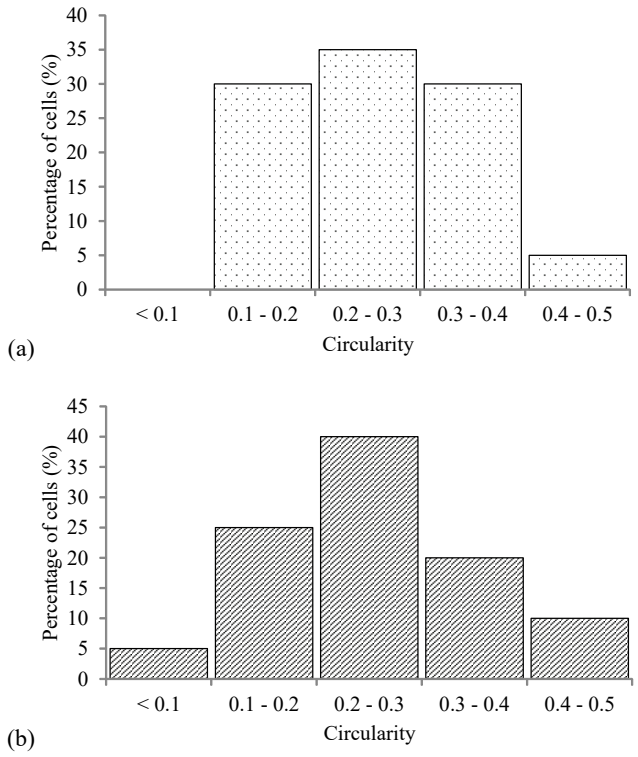

Fig. 11. Frequency distribution of cell circularity in (a) sparse zone (SD: 0.09) and (b) dense zone (SD: 0.1)

4. Discussion

In this paper, the cells have been successfully guided to migrate from the sparse zone to the dense zone. The cell polarization angle plays an important role in the guided cell migration. The cell polarization angle has been quantified in both the sparse zone and the dense zone. It can be seen that the micropillar substrate significantly affects the cell polarization angle in different zones. The average polarization angle in the sparse zone is only 26° while the average polarization angle in the dense zone is 60°. This indicates that the cells are oriented in the direction of the space gradient in the sparse zone, which is also the cell migration direction.

One-way ANOVA was used to determine the significance in the difference of the cell aspect ratios on the micropatterned surface and the flat surface. The *p*-values are 0.3, 0.8, 0.1 and 0.2 at the spacing gradients of 0.1, 0.2, 0.3 and 0.4, respectively. The lack of statistical significance indicates that the cells have similar levels of attachment to the micropatterned surfaces, as they have to flat surfaces. One-way ANOVA, with an assumed confidence level of 95%, was used to compare the cell circularity on the graded micropillar surface and the flat surface. The cells on the flat surface have an average circularity of 0.3, which is similar to other reported circularity for 3T3 fibroblasts [13]. It is found that for the smaller micropillar diameters of 5 μm and 10 μm, the *p*-values are less than 0.05, representing a significant increase in the average circularity compared to the flat surface. However, for the larger micropillar diameters of 15 μm and 20 μm, the *p*-values are greater than 0.05, indicating no significant difference in the cell circularity compared to the flat surface. There are two possible reasons. Larger micropillars offer greater areas for the cells to attach and elongate, with a similar effect to the cell spreading on the flat surface. The filopodia from the leading edge of the cells have greater space to attach on the neighboring micropillars. The cells may have a physiological limit beyond which the cells sense the underlying microtopographic surface as a flat surface. Moreover, it is reported that the cells attach better on stiffer substrates [24]. In this study, the cells attach on the graded micropillar substrate. The stiffness of the micropillar substrate is proportional to the fourth power of the micropillar diameter. Hence, the cells have reduced circularities due to better attachment on the larger micropillars.

Guided cell migration in this study is a unique phenomenon due to the responses of cells to underlying topography. By tailoring the local topographic environment, the cells are successfully guided to migrate in a preferred direction. There are several potential applications of guided cell migration including cell sorting, wound healing, cancer cell detection and grading, to name a few. For example, different types of cells have different migration behaviors due to their different stiffnesses. By optimizing the topographic parameters, mixture of multiple types of cells can be separated. In addition, cancer grade is a critical factor in the diagnosis and subsequent treatment, which describes how abnormal the cells are compared to normal and healthy cells, and is of great importance in determining the prognosis, and the nature and intensity of treatment path. Cancerous mutations cause an alteration in the stiffness of cells through change of internal protein scaffolds within the cells. The increased cellular stiffness has been directly correlated with cancer aggressiveness, which results in different migration behaviors on the micropillar substrates. By adding the chemoattractant, the fibroblasts are guided to migrate towards the wounds aiming at wound healing.

5. Conclusions

In this study, a graded micropillar substrate has been fabricated to investigate the effect of the micro-

topography on the cell morphology in terms of the cell aspect ratio and cell circularity. Cell aspect ratio represents the ratio of the longest cell length to the shortest length. A higher cell aspect ratio implies better cell attachment and proliferation performance. With the increase of the micropillar diameter, the cell aspect ratio has no significance change. At the small spacing gradients, the aspect ratio is smaller than that at the large spacing gradients. Statistical analysis shows that both the micropillar diameter and spacing gradient have no significant effect on the cell aspect ratio compared to the flat surface. Cell circularity reflects the shape of the cells. A circularity of 1 implies that the cells have not attached, while cell circularities smaller than 1 imply the attachment of cells. The cell circularity at the small micropillar diameters is higher than that at the large micropillar diameters. The cell circularity at the micropillar gradient of 0.1 μm is higher than those at the other micropillar gradients. Three microtopographic conditions are considered to have statistically significant effects on the cell circularity compared to the flat surface, including the micropillar diameters of 5 μm and 10 μm and the spacing gradient of 0.1 μm. Future work may involve the tailoring of the micropillar substrates to induce cell patterning and cell sorting.

Acknowledgements

This work was partially supported by Texas Tech University startup fund, and National Natural Science Foundation of China (51709120).

References

[1] ALAPAN Y., YOUNESI M., AKKUS O., GURKAN U.A., *Anisotropically stiff 3D micropillar niche induces extraordinary cell alignment and elongation*, Adv. Healthc. Mater., 2016, 5, 1884–1892.

[2] BEUSSMAN K.M., RODRIGUEZ M.L., LEONARD A., TAPARIA N., THOMPSON C.R., SNIADECKI N.J., *Micropost arrays for measuring stem cell-derived cardiomyocyte contractility*, Methods, 2016, 94, 43–50.

[3] CROUCH A.S., MILLER D., LUEBKE K.J., HU W., *Correlation of anisotropic cell behaviors with topographic aspect ratio*, Biomaterials, 2009, 30, 1560–1567.

[4] DALBY M.J., GADEGAARD N., RIEHLE M.O., WILKINSON C.D., CURTIS A.S., *Investigating filopodia sensing using arrays of defined nano-pits down to 35 nm diameter in size*, Int. J. Biochem. Cell B., 2004, 36, 2005–2015.

[5] FANG M., GOLDSTEIN E.L., TURNER A.S., LES C.M., ORR B.G., FISHER G.J., WELCH K.B., ROTHMAN E.D., BANASZAK HOLL M.M., *Type I collagen D-spacing in fibril bundles of dermis, tendon, and bone: bridging between nano-and micro-level tissue hierarchy*, ACS Nano, 2012, 6, 9503–9514.

[6] FENG J.F., LIU J., ZHANG X.Z., ZHANG L., JIANG J.Y., NOLTA J., ZHAO M., *Guided migration of neural stem cells derived from human embryonic stem cells by an electric field*, Stem Cells, 2012, 30, 349–355.

[7] FRANTZ C., STEWART K.M., WEAVER V.M., *The extracellular matrix at a glance*, J. Cell Sci., 2010, 123, 4195–4200.

[8] GHIBAUDO M., SAEZ A., TRICHET L., XAYAPHOUMMINE A., BROWAE S.J., SILBERZAN P., BUGUIN A., LADOUX B., *Traction forces and rigidity sensing regulate cell functions*, Soft Matter, 2008, 4, 1836–1843.

[9] HUI J., PANG S.W., *Cell migration on microposts with surface coating and confinement*, Biosci. Rep., 2019, 39, BSR20181596.

[10] JACQUEMET G., HAMIDI H., IVASKA J., *Filopodia in cell adhesion, 3D migration and cancer cell invasion*, Curr. Opin. Cell Biol., 2015, 36, 23–31.

[11] KIM D.H., HAN K., GUPTA K., KWON K.W., SUH K.Y., LEVCHENKO A., *Mechanosensitivity of fibroblast cell shape and movement to anisotropic substratum topography gradients*, Biomaterials, 2009, 30, 5433–5444.

[12] KRISHNAMOORTHY S., NOORANI B., XU C., *Effects of encapsulated cells on the physical–mechanical properties and microstructure of gelatin methacrylate hydrogels*, Int. J. Mol. Sci., 2019, 20, 5061.

[13] MANCIA A., ELLIOTT J.T., HALTER M., BHADRIRAJU K., TONA A., SPURLIN T.A., MIDDLEBROOKS B.L., BAATZ J.E., WARR G.W., PLANT A.L., *Quantitative methods to characterize morphological properties of cell lines*, Biotechnol. Prog., 2012, 28, 1069–1078.

[14] NIE F.Q., YAMADA M., KOBAYASHI J., YAMATO M., KIKUCHI A., OKANO T., *On-chip cell migration assay using microfluidic channels*, Biomaterials, 2007, 28, 4017–4022.

[15] NGUYEN A.T., SATHE S.R., YIM E.K., *From nano to micro: topographical scale and its impact on cell adhesion, morphology and contact guidance*, J. Condens. Matter Phys., 2016, 28, 183001.

[16] PAINTER K.J., *Continuous models for cell migration in tissues and applications to cell sorting via differential chemotaxis*, Bull. Math. Biol., 2009, 71, 1117.

[17] PARK J., KIM D.H., KIM H.N., WANG C.J., KWAK M.K., HUR E., SUH K.Y., AN S.S., LEVCHENKO A., *Directed migration of cancer cells guided by the graded texture of the underlying matrix*, Nat. Mater., 2016, 15, 792–801.

[18] PARK J., KIM D.H., LEVCHENKO A., *Topotaxis: a new mechanism of directed cell migration in topographic ECM gradients*, Biophys. J., 2018, 114, 1257–1263.

[19] PETERBAUER T., HEITZ J., OLBRICH M., HERING S., *Simple and versatile methods for the fabrication of arrays of live mammalian cells*, Lab Chip, 2006, 6, 857–863.

[20] PRAGER-KHOUTORSKY M., LICHTENSTEIN A., KRISHNAN R., RAJENDRAN K., MAYO A., KAM Z., GEIGER B., BERSHADSKY A.D., *Fibroblast polarization is a matrix-rigidity-dependent process controlled by focal adhesion mechanosensing*, Nat. Cell Biol., 2011, 13, 1457.

[21] RIDLEY A.J., SCHWARTZ M.A., BURRIDGE K., FIRTEL R.A., GINSBERG M.H., BORISY G., PARSONS J.T., HORWITZ A.R., *Cell migration: integrating signals from front to back*, Science, 2003, 302, 1704–1709.

[22] XU C., ZHANG Z., CHRISTENSEN K., HUANG Y., FU J., MARKWALD R.R., *Freeform vertical and horizontal fabrication of alginate-based vascular-like tubular constructs using inkjetting*, J. Manuf. Sci. Eng., 2014, 136, 061020.

[23] Xu H., Casillas J., Krishnamoorthy S., Xu C., *Effect of Irgacure 2959 and lithium phenyl-2, 4, 6-trimethylbenzoyphosphinate on cell viability, physical properties, and microstructure in 3D bioprinting of vascular-like constructs*, Biomed. Mater., 2020, 15, 055021.

[24] Yeung T., Georges P.C., Flanagan L.A., Marg B., Ortiz M., Funaki M., Zahir N., Ming W., Weaver V., Janmey P.A., *Effects of substrate stiffness on cell morphology, cytoskeletal structure, and adhesion*, Cell Motil. Cytoskel., 2005, 60, 24–34.